Silicon Microtoroidal Resonators With Integrated MEMS Tunable Coupler

Jin Yao, David Leuenberger, Ming-Chang M. Lee, *Member, IEEE*, and Ming C. Wu, *Fellow, IEEE*

***Abstract*—A single crystalline silicon microtoroidal resonator with integrated MEMS-actuated tunable optical coupler is demonstrated for the first time. It is fabricated by combining hydrogen annealing and wafer bonding processes. The device operates in all three coupling regimes: under-, critical, and over-coupling. We have also developed a comprehensive model based on time-domain coupling theory. The experimental and theoretical results agree very well. The quality factor (Q) is extracted by fitting the experimental curve with the model. The unloaded Q is as high as 110 000, and the loaded Q is continuously tunable from 110 000 to 5400. The extinction ratio of the transmittance is 22.4 dB. This device can be used as a building block of resonator-based reconfigurable photonic integrated circuits.**

***Index Terms*—Integrated optics, optical resonators, surface roughness, tunable.**

I. Introduction

OPTICAL microresonators are key enabling elements for compact filters [1], lasers [2], electro-optic modulators [3], add–drop multiplexers [4], optical dispersion compensators [5], delay lines [6], nonlinear optical devices [7], and optical sensors [8], [9]. The performance of microresonators depends on two parameters: the quality factor (Q) of the resonator and the coupling ratio between the waveguides and the resonator (κ). Microfabricated resonators with very high Q has been demonstrated in SiO_2 [10] and Si [11]. The coupling ratio needs to be controlled precisely to achieve optimum performance [12]. This has been achieved by adjusting prism couplers in fused silica microsphere resonators [13] or by moving tapered fiber couplers [14]–[16] with piezo-controlled micropositioners. However, such setups are bulky and cannot be integrated. In microresonators with integrated waveguides, the coupling ratio is determined by the fabrication process [17]. The value of κ or, perhaps more importantly, its relation with the cavity Q, cannot be controlled precisely. Some trimming processes have been proposed to control the resonance frequency, but not κ [18], [19].

Recently, microresonators with tunable coupling ratios have been reported [20]–[23]. A Mach–Zehnder interferometer (MZI) has been integrated with a racetrack resonator [20]. The resonator can operate in all coupling regimes (uncoupled, under-, critical, or over-coupled). An unloaded Q of 1.9×10^4 and an On–Off ratio of 18.5 dB have been achieved. However, the circumference of the resonator is rather large (1430 μm) due to the long MZI structure, which limits the free spectral range and the footprint that it can achieve. Recently, microfluidic approach has also been employed to tune both the resonance wavelength and the coupling ratio of low-index microring resonators made in SU8 [23]. The refractive index of the surrounding media was varied by mixing two different liquids. Critical coupling with an extinction ratio of 37 dB have been attained. However, index variation is small (~ 0.04), which limits the tuning range of κ. In addition, the tuning speed is slow ($\sim 2\,\mathrm{s}$) and the fluidic packaging is cumbersome.

Previously, we have reported the first silicon microdisk resonator with integrated microelectromechanical systems (MEMS) tunable coupler [21], [22]. By physically changing the gap spacing between the waveguide and the resonator, κ can be varied over a wide range (0 to 34%) and a high Q (100 000) have been achieved simultaneously. Tunable dispersion compensators (185 to 1200 ps/nm) have also been demonstrated [22]. One drawback of that device is the lack of radial mode control in microdisk resonators, which could produce additional resonances due to high-order modes. In this paper, we report on the first single crystalline silicon *microtoroidal* resonator with MEMS tunable optical coupler. Microtoroidal resonators offer tighter confinement of the optical mode and eliminate multiple radial modes observed in microdisks. Microtoroidal resonators have been made in SiO_2 by thermal reflow [10], however, such process cannot be applied to single crystalline structures. Instead, we use hydrogen annealing to create three-dimensional toroidal structures while preserving the single crystalline quality [24]. To integrate the microtoroidal resonators with MEMS tunable waveguides, we have combined the hydrogen annealing process with wafer bonding technique. All the three coupling regimes have been demonstrated, with the loaded Q tunable from 110 000 to 5400.

II. Device Design and Fabrication

A. Device Structure Design

The schematic of the tunable microtoroidal resonator is shown in Fig. 1. Two suspended waveguides are vertically coupled to a microtoroidal resonator. It is realized on a two-layer silicon-on-insulator (SOI) structure. The microtoroid and the fixed electrodes of the MEMS actuators are fabricated on the lower SOI layer, while the suspended waveguides are integrated on the upper SOI. The initial spacing between the microtoroid and the

Manuscript received October 2, 2006; revised February 12, 2007. This work was supported in part by the Defense Advanced Research Project Agency (DARPA) University Photonics Research (UPR) Program HR0011-04-1-0040. The work of D. Leuenberger was supported by a one-year fellowship from the Swiss National Science Foundation, in 2005.

J. Yao and M. C. Wu are with the Department of Electrical Engineering and Computer Sciences, University of California, Berkeley, CA 94720 USA (e-mail: jinyao@eecs.berkeley.edu; wu@eecs.berkeley.edu).

D. Leuenberger is with the Integrated Photonics Laboratory, University of California, Berkeley, CA 94720 USA (e-mail: dleuen@eecs.berkeley.edu).

M.-C. M. Lee is with the Department of Electrical Engineering and the Institute of Photonics Technologies, National Tsing Hua University, Hsinchu 30055, Taiwan, R.O.C. (e-mail: mclee@ee.nthu.edu.tw).

Digital Object Identifier 10.1109/JSTQE.2007.893743

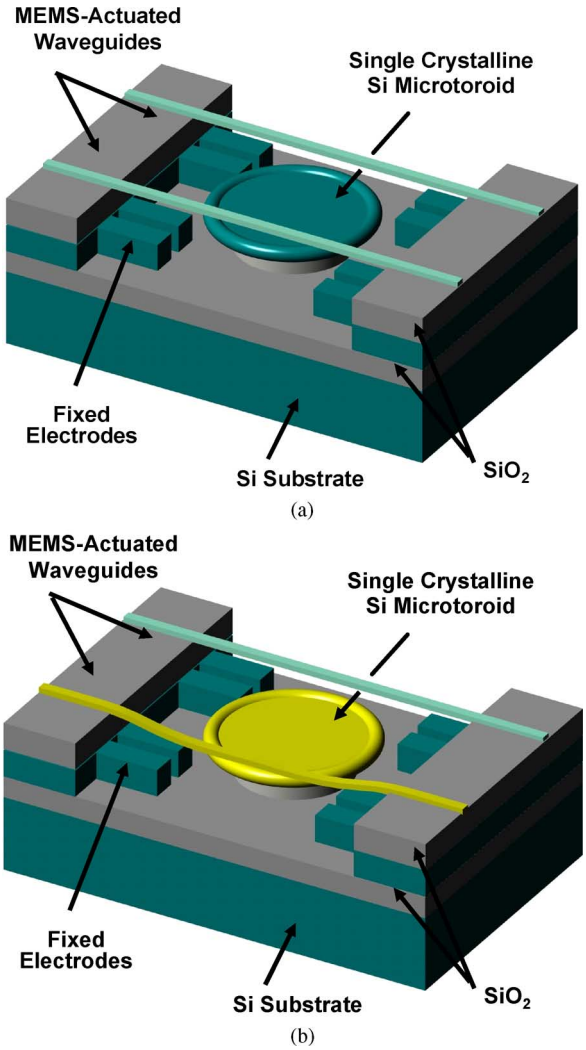

Fig. 1. (a) Schematic of the microtoroidal resonator with integrated MEMS tunable couplers. At zero bias, the initial spacing is large enough to ensure negligible coupling between the resonator and the waveguide coupler. (b) Schematic of the microtoroidal resonator with integrated MEMS tunable couplers under biased actuation. Lower waveguide is pulled downward to increase coupling, while the upper waveguide remains straight (uncoupled).

waveguides is 1 μm. It is chosen so that there is negligible coupling at zero bias, as shown in Fig. 1(a). With increasing voltage bias between the waveguide and the fixed electrodes, the suspended waveguide is pulled down toward the microtoroid, increasing the optical coupling exponentially, as illustrated in Fig. 1(b).

This design enables us to bias the microtoroidal resonator in all coupling regimes: under-coupling, critical coupling, and over-coupling, or even decoupled from the waveguide bus. Details of the MEMS actuator design have been reported in [22].

There is a design tradeoff in the doping concentration of the Si device layers. High doping is desired for the MEMS actuation, while low doping is necessary to minimize the optical absorption due to free carriers. Fortunately, electrostatic actuation does not require low resistivity. With a doping concentration of 10^{14} cm^{-3} (n-type dopants), a resistivity of 10 Ω·cm and an optical loss smaller than 0.01 cm^{-1} can be achieved. This absorption

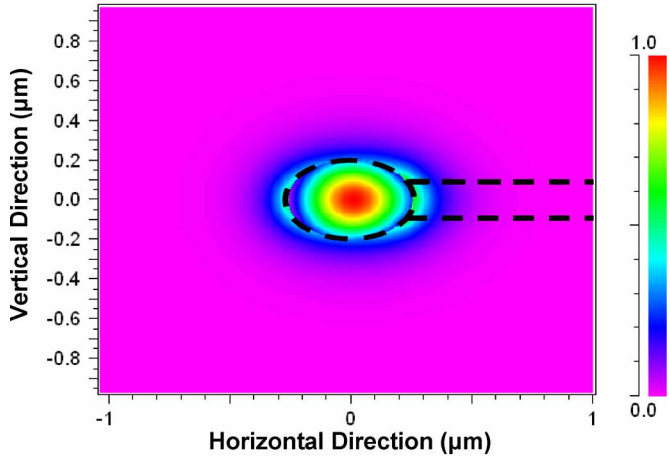

Fig. 2. Optical mode profile of the toroid for TE-like polarized light at 1.55 μm.

coefficient corresponds to a Q of 10^8 for microresonators if it is the dominant loss.

B. Waveguide Design for Phase Matching

Phase matching between the waveguide and the resonator is important to achieve an efficient coupling. Phase matching is satisfied when the two wave modes have the same propagation constant β.

We calculated the propagation constants of the microtoroid with the actual shape produced by hydrogen annealing using beam propagation method (BPM).[1] The optical field profile of the toroidal resonator at 1.55-μm wavelength is shown in Fig. 2. We used the following parameters in the calculation: refractive indexes of Si and air are 3.46 and 1.0, respectively; the bend radius of the toroid is 19.5 μm; and the radius of the toroid is 200 nm. It supports only one TE-like optical mode tightly confined to silicon.

Phase matching is achieved by controlling the dimensions of the waveguide. Fig. 3 shows the calculated propagation constants of the waveguide (lines) and the microtoroid (dots) versus wavelength for various waveguide dimensions. Here, we fix the waveguide width at 0.69 μm, the smallest linewidth that can regularly be produced by our lithography tool (10:1 reduction stepper). As shown in Fig. 3, the waveguide with 0.25-μm thickness is best matched to the microtoroid mode over a wide wavelength range around 1550 nm.

C. Fabrication Process

Our vertically coupled tunable microresonator was fabricated on a two-layer SOI using the wafer bonding process. The main challenge, here, was the nonplanar topography of the microtoroids that prevents the tight contact necessary for wafer bonding. We solved this problem by thinning the edges of the microdisks before hydrogen annealing so that the microtoroid surface was lower than the surrounding planar area. The detailed

[1]http://www.rsoftdesign.com/products/component_design/BeamPROP/

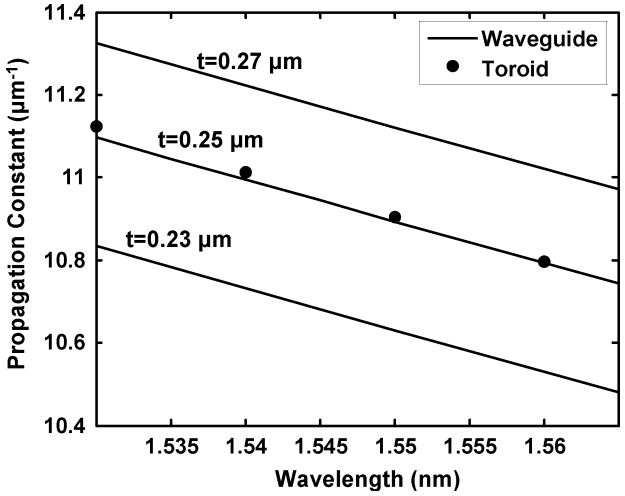

Fig. 3. Calculated propagation constants of the waveguide and the microtoroid versus wavelengths for various waveguide thicknesses, t. The width of the waveguide is fixed at 0.69 μm.

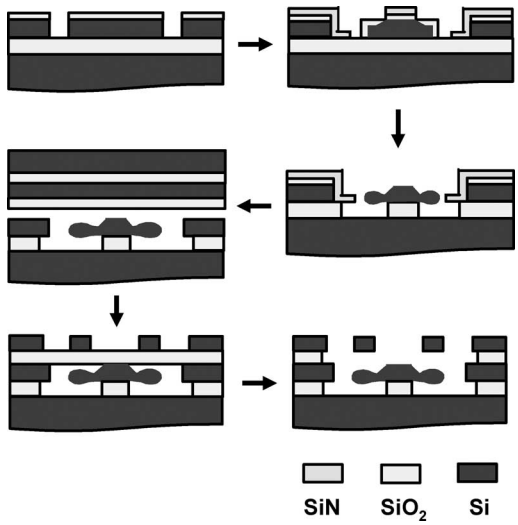

Fig. 4. Fabrication process for the tunable microtoroidal resonator.

fabrication process is shown in Fig. 4. First, microdisks were patterned and etched on an SOI wafer with a 350-nm-thick device layer. The edges of the disks were thinned down to 200 nm by thermal oxidation. This allowed room for the microtoroids to expand in the vertical direction during hydrogen annealing. The sample was then partially released in buffered HF and annealed in 10-Torr hydrogen ambient at 1050 °C for 5 min, creating a toroidal rim around the disks. The hydrogen annealing condition was optimized for the formation of the microtoroids, as reported in [24], [25]. A second SOI wafer with a 700-nm-thick device layer was thermally oxidized to create a SiO_2 spacer of 1-μm thickness. After oxidation, the thickness of the device layer was reduced to 250 nm. The toroid wafer was then fusion-bonded to the SOI wafer, whose substrate was subsequently removed to reveal the second SOI layer. The microtoroids were visible through the thin SOI layer, and the waveguide patterns were aligned to the edges of the underneath microtoroids. Finally, the waveguides around the toroids were released in buffered HF and supercritical dryer. In addition to creating a toroidal shape, the hydrogen annealing also reduced the surface roughness (to < 0.26 nm as reported in [26]), which was critical to attain high Q.

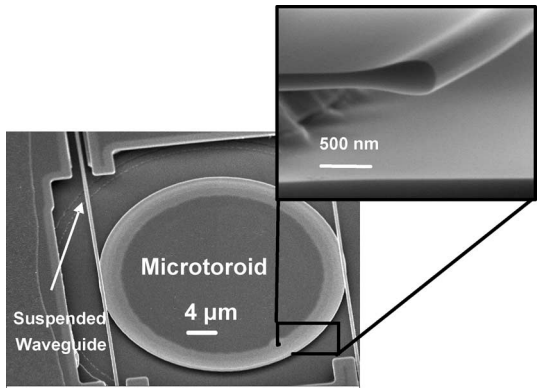

Fig. 5. SEM of the microtoroidal resonator and the suspended waveguides. Inset shows the cross-sectional view of the microtoroid.

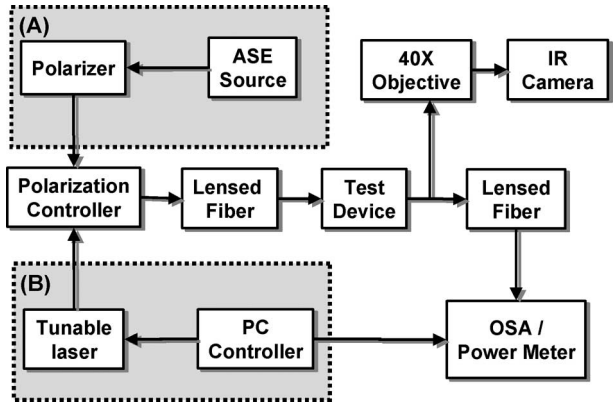

Fig. 6. Experimental setup for optical characterization. Amplified spontaneous emission (ASE) source is used (a) for quick measurement of the spectral response and (b) while the tunable laser provides high-resolution characterization.

The scanning electron micrograph (SEM) of the fabricated device is shown in Fig. 5. The dimensions of the waveguides are measured to be 0.69-μm wide and 0.25-μm thick, very close to the designed parameters. The resonator exhibits a very smooth sidewall.

III. Optical Characterization

The optical performance of the tunable microtoroidal resonator is tested using either a broadband amplified spontaneous emission (ASE) source (OpticWave Mini BLS-C-13) or a tunable laser (Agilent 81680A), as shown in Fig. 6. Light is coupled to the waveguides by polarization-maintaining lensed fibers. A calibrated optical power meter (HP 8153A) and an optical spectrum analyzer (OSA) (ANDO AQ6317B) are placed at the output to measure the transmitted power. The ASE provides a broadband source for quick measurement over a wide spectral range, while the tunable laser is used for high-resolution characterization. We have used TE-polarized input, which is attained by a linear polarizer and a polarization controller.

To actuate the waveguide, a voltage bias is applied to the fixed electrodes while the waveguide is grounded. At zero bias, almost

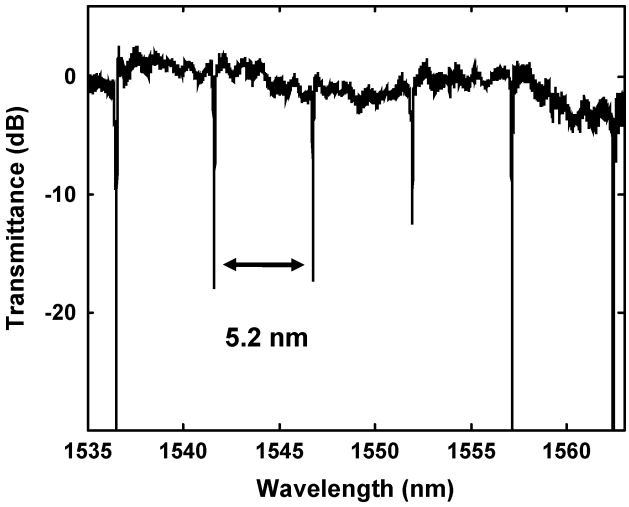

Fig. 7. Measured optical spectrum of a microtoroidal resonator at a bias voltage of 67 V. Measured free spectral range (FSR) of the TE mode is 5.2 nm.

100% of the light is transmitted to the output port. With increasing bias, sharp dips gradually appear in the transmission spectrum (Fig. 7). Each dip corresponds to a resonance wavelength. The free spectral range (FSR) of the TE mode is measured to be 5.2 nm. The small ripples are due to the reflections from the cleaved facets (Fabry–Perot effect). They can be eliminated by antireflection coating of the facets. Only a resonance peak is observed within each FSR, confirming the successful suppression of multiple radial modes observed in microdisk resonators.

The integrated tunable coupler enables the microresonator to operate in all coupling regimes. At low voltage, the microresonator is under-coupled. Fig. 8(a) shows the normalized transmission spectra of the resonator around one of the resonant wavelengths at 1548.2 nm at bias voltages of 51.0, 56.0, and 64.8 V. As the voltage increases, the optical coupling becomes stronger, leading to a larger dip at resonance. The three coupling regimes are clearly visible in Fig. 8(b), which plots the normalized transmittance at the resonant wavelength changes as a function of the applied voltage. In the under-coupling regime ($V_{\rm bias} < 114$ V), the transmittance decreases continuously with the increasing voltage. The transmittance reaches a minimum at critical coupling ($V_{\rm bias} = 114$ V). The extinction ratio is measured to be 22.4 dB at critical coupling. Further increase in voltage moves the resonator into the over-coupling regime. The increase in transmittance is accompanied by a broadening of the resonance linewidth since the coupling to waveguide is now stronger than the intrinsic loss of the resonator.

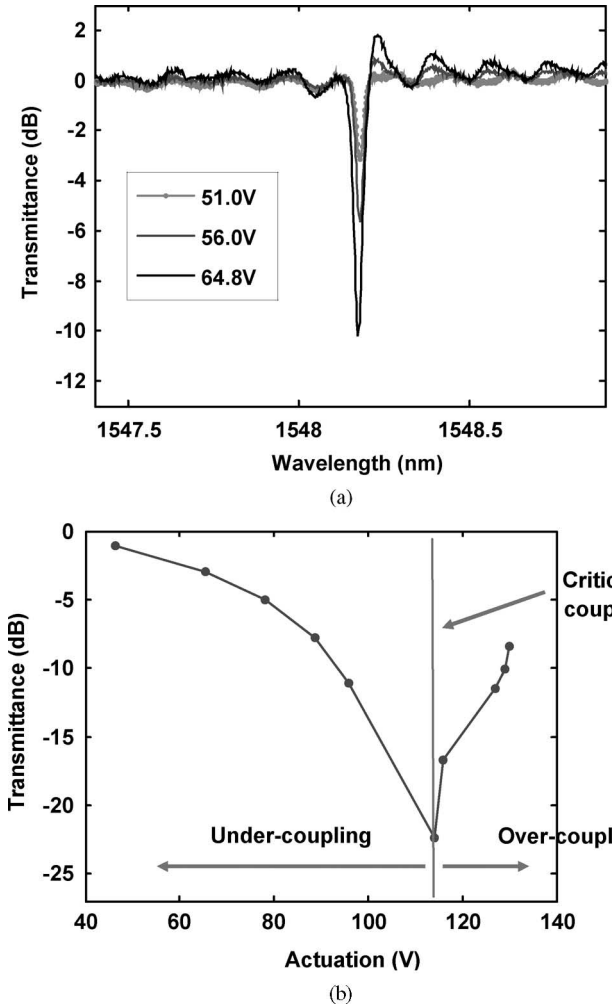

Fig. 8. (a) Measured normalized optical spectra of a microtoroidal resonator at bias voltages of 51.0, 56.0, and 64.8 V. (b) Normalized transmittance at resonance versus actuation voltage. Microresonator can be tuned continuously from under-coupling regime to over-coupling regime.

IV. Theoretical Modeling and Analysis

According to the time-domain coupling theory [1], the optical transfer function of the microresonator can be expressed as a function of resonant frequency (ω_0) and amplitude decay time constants τ_0 and τ_e, due to intrinsic loss and external coupling respectively

$$t_{\rm res} = \frac{j(\omega-\omega_0) + \frac{1}{\tau_0} - \frac{1}{\tau_e}}{j(\omega-\omega_0) + \frac{1}{\tau_0} + \frac{1}{\tau_e}} \tag{1}$$

where $t_{\rm res}$ is the amplitude transfer function of the microresonator.

Alternatively, the transfer function can also be expressed in terms of the unloaded quality factor Q_0 and the external quality factor Q_e

$$t_{\rm res} = \frac{2j\left(\frac{\lambda_0-\lambda}{\lambda}\right) + \left(\frac{2}{Q_0} - \frac{1}{Q_L}\right)}{2j\left(\frac{\lambda_0-\lambda}{\lambda}\right) + \left(\frac{1}{Q_L}\right)} \tag{2}$$

where $Q_0 = \omega_0\tau_0/2$, $Q_e = \omega_0\tau_e/2$, and the loaded quality factor Q_L is defined as

$$\frac{1}{Q_L} = \frac{1}{Q_0} + \frac{1}{Q_e} \tag{3}$$

The measured spectra are usually complicated by the Fabry–Perot resonance between the two cleaved facets, as illustrated in Fig. 9. To model the measured spectrum more precisely, and extract the Q values of the resonator more accurately, particularly when the resonance peak is small, we develop a comprehensive

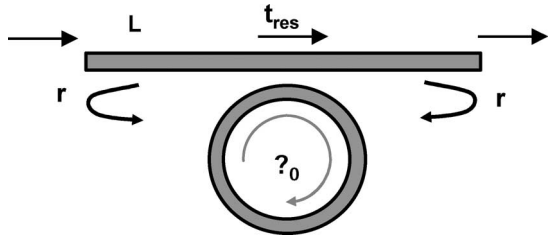

Fig. 9. Schematics illustrating the interaction between the microresonator and the Fabry–Perot resonance of the coupling waveguide.

model that includes both the effect of the microresonator and the Fabry–Perot ripples.

The total transmission $t_{\rm tot}$ is now a summation of multiple transmissions through the waveguide, as shown in

$$\begin{aligned} t_{\rm tot} &= (1-r)^2 \exp(-\alpha L)\exp(jkLn_{\rm eff})t_{\rm res} \\ &\quad + (1-r)^2 r^2 \exp(-3\alpha L)\exp(j(3kLn_{\rm eff}+2\phi_{\rm R}))t_{\rm res}^3 \\ &\quad + (1-r)^2 r^4 \exp(-5\alpha L)\exp(j(5kLn_{\rm eff}+4\phi_{\rm R}))t_{\rm res}^5 \\ &\quad + L \end{aligned} \tag{4}$$

where r is the amplitude reflection coefficient at the facet of the silicon waveguide, α is the optical loss per unit length in the waveguide, L is the length of the waveguide, k is the free-space propagation constant, $n_{\rm eff}$ is the effective refractive index of the Si waveguide, and $\phi_{\rm R}$ is the optical phase change at the reflection per interface. Since there is a π phase shift at the reflection interface, the total transmission $t_{\rm tot}$ can be simplified to

$$\begin{aligned} t_{\rm tot} &= (1-r)^2 \exp(-\alpha L)\exp(jkLn_{\rm eff})t_{\rm res} \\ &\quad \{1 + r^2 \exp(-2\alpha L)\exp(j2kLn_{\rm eff})t_{\rm res}^2 \\ &\quad + r^4 \exp(-4\alpha L)\exp(j4kLn_{\rm eff})t_{\rm res}^4 + L\} \\ &= a_0(1+q+q^2+q^3+L) \\ &= \frac{a_0}{1-q} \end{aligned} \tag{5}$$

where $a_0 = (1-r)^2 \exp(-\alpha L)\exp(jkLn_{\rm eff})t_{\rm res}$, and $q = r^2 \exp(-2\alpha L)\exp(j2kLn_{\rm eff})t_{\rm res}^2$.

In this derivation, we have assumed that the backscattering effect is small and can be neglected. The total intensity transmittance is then given by

$$T_{\rm res} = |t_{\rm tot}|^2 \tag{6}$$

To include the effect of waveguide dispersion, the phase factor $kLn_{\rm eff}$ is replaced by

$$\begin{aligned} \phi &= kL\left[n_{\rm eff} + \frac{dn}{d\lambda}(\lambda-\lambda_0)\right] \\ &= kLn_{\rm eff}\left[1 + \frac{dn}{d\lambda}\frac{1}{n_{\rm eff}}(\lambda-\lambda_0)\right] \\ &= kLn_{\rm eff}\left[1 + D_\lambda(\lambda-\lambda_0)\right] \end{aligned} \tag{7}$$

where $D_\lambda = \frac{dn}{d\lambda}\frac{1}{n_{\rm eff}}$.

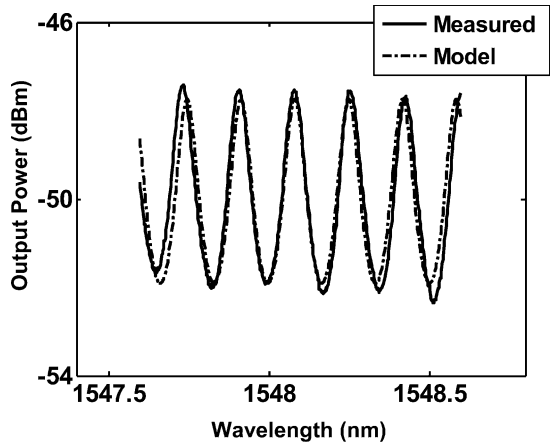

(a)

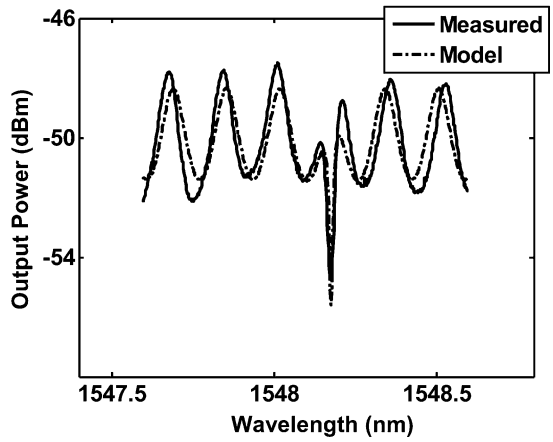

(b)

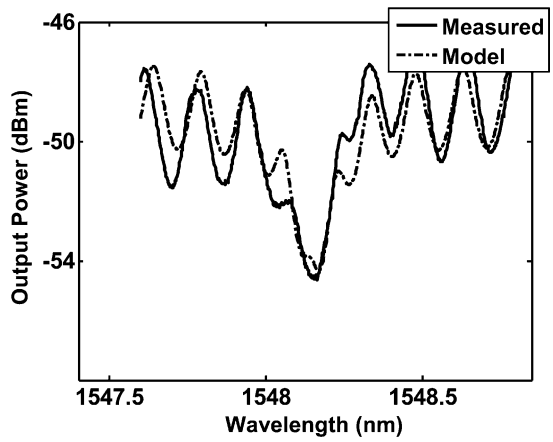

(c)

Fig. 10. (a) Measured and modeled spectra at 0 V (microresonator is decoupled). (b) Measured and modeled spectra at 64.8 V (microresonator is undercoupled). (c) Measured and modeled spectra at 130 V (microresonator is overcoupled).

The quality factors Q_0 and Q_L are extracted from the measured optical spectra by least-mean-square-error fitting to the model. Fig. 10 shows the measured and the fitted spectra around the resonance peak at 1548.2 nm when the resonator is:

a) decoupled; b) under-coupled; and c) over-coupled. The experimental data agree very well with the theoretical model. From the fitted spectral response, the unloaded quality factor Q_0 of the microtoroidal resonator is extracted to be 110 000. The loaded Q, i.e., Q_L, is continuously tunable from 110 000 to 5400, exhibiting a tuning ratio of more than 20:1.

The model described in this paper fit not only the resonance peak but also the ripples due to Fabry–Perot resonance. The quality factor extracted by this method is more accurate than by the lumped resonator model alone [27], especially when the resonance peak is small.

V. Discussion

Hydrogen annealing is a simple and powerful technique to fabricate suspended microring resonators with high-quality factor and single radial mode. Comparing the etched ring with tethered anchor [17], the seamless toroidal structure has lower scattering loss and higher Q. The hydrogen annealing process also greatly reduces the surface roughness, as confirmed by the high Q measured in our devices. These tunable microresonators described in this paper can be cascaded to form reconfigurable optical add–drop multiplexers, wavelength-selective switches, and crossconnects. It can also be used for bandwidth-tunable filters in dynamic optical networks. With the successful suppression of multiple radial modes, we expect the microtoroidal resonator to have even larger bandwidth tuning ratio than the microdisk-based filters in [28].

VI. Conclusion

We have successfully demonstrated a novel single crystalline silicon microtoroidal resonator with MEMS-actuated tunable optical coupler. It is fabricated by combining the hydrogen annealing and the wafer bonding processes. We have achieved an unloaded Q of 110 000 for a 39-μm-diameter resonator with a toroidal radius of 200 nm. The device is able to operate in all the three coupling regimes: under-, critical, and over-coupling. The resonator can also be decoupled from the waveguide, allowing them to be cascaded without loading the waveguides. We have developed a detailed model combining the time-domain coupling theory with the Fabry–Perot resonance of the waveguide. The experimental and the theoretical results agree very well. The loaded Q is continuously tunable from 110 000 to 5400. This device has potential applications in variable-bandwidth filters, reconfigurable add–drop multiplexers, wavelength-selective switches and crossconnects, and optical sensors.

Acknowledgment

The authors would like to thank the staff of the Microfabrication Laboratory, University of California, Berkeley. Part of the fabrication process was performed at Stanford Nanofabrication Facility, Stanford University. In particular, they would also like to acknowledge the assistance of M. Stevens and M. Mansourpour. They would also like to thank Dr. S. Mathai of the University of California, Berkeley, for helpful discussions and technical assistance.

References

[1] B. E. Little, S. T. Chu, H. A. Haus, J. Foresi, and J. P. Laine, "Microring resonator channel dropping filters," *J. Lightw. Technol.*, vol. 15, no. 6, pp. 998–1005, Jun. 1997.

[2] S. J. Choi, K. Djordjev, S. J. Choi, and P. D. Dapkus, "Microdisk lasers vertically coupled to output waveguides," *IEEE Photon. Technol. Lett.*, vol. 15, no. 10, pp. 1330–1332, Oct. 2003.

[3] Q. Xu, B. Schmidt, S. Pradhan, and M. Lipson, "Micrometre-scale silicon electro-optic modulator," *Nature*, vol. 435, no. 7040, pp. 325–327, May 2005.

[4] B. E. Little, S. T. Chu, W. Pan, and Y. Kokubun, "Microring resonator arrays for VLSI photonics," *IEEE Photon. Technol. Lett.*, vol. 12, no. 3, pp. 323–325, Mar. 2000.

[5] C. K. Madsen, G. Lenz, A. J. Bruce, M. A. Cappuzzo, L. T. Gomez, T. N. Nielsen, L. E. Adams, and I. Brenner, "An all-pass filter dispersion compensator using planar waveguide ring resonators," in *Proc. Opt. Fiber Commun. Conf. Int. Conf. Integr. Opt. Opt. Fiber Commun. (OFC/IOOC)*, Piscataway, NJ, Feb. 1999, vol. 4, pp. 99–101.

[6] G. Lenz, B. J. Eggleton, C. K. Madsen, and R. E. Slusher, "Optical delay lines based on optical filters," *IEEE J. Quantum Electron.*, vol. 37, no. 4, pp. 525–532, Apr. 2001.

[7] T. J. Kippenberg, S. M. Spillane, D. K. Armani, and K. J. Vahala, "Ultralow-threshold microcavity Raman laser on a microelectronic chip," *Opt. Lett.*, vol. 29, pp. 1224–1227, Jun. 2004.

[8] F. Vollmer, S. Arnold, D. Braun, I. Teraoka, and A. Libchaber., "Multiplexed DNA quantification by spectroscopic shift of two microsphere cavities," *Biophys. J.*, vol. 85, pp. 1974–1979, Sep. 2003.

[9] A. M. Armani and K. J. Vahala, "Heavy water detection using ultra-high-Q microcavities," *Opt. Lett.*, vol. 31, no. 12, pp. 1896–1898, Jun. 2006.

[10] D. K. Armani, T. J. Kippenberg, S. M. Spillane, and K. J. Vahala, "Ultra-high-Q toroid microcavity on a chip," *Nature*, vol. 421, pp. 925–929, Feb. 2003.

[11] M. Borselli, T. Johnson, and O. Painter, "Beyond the Rayleigh scattering limit in high-Q silicon microdisks: theory and experiment," *Opt. Express*, vol. 13, no. 5, pp. 1515–1530, Mar. 2005.

[12] A. Yariv, "Critical coupling and its control in optical waveguide-ring resonator systems," *IEEE Photon. Technol. Lett.*, vol. 14, no. 4, pp. 483–485, Apr. 2002.

[13] V. B. Braginsky, M. L. Gorodetsky, and V. S. Ilchenko, "Quality-factor and nonlinear properties of optical whispering-gallery modes," *Phys. Lett. A*, vol. 137, pp. 393–397, May 1989.

[14] J. C. Knight, G. Cheung, F. Jacques, and T. A. Birks, "Phase-matched excitation of whispering-gallery-mode resonances by a fiber taper," *Opt. Lett.*, vol. 22, pp. 1129–1131, Aug. 1997.

[15] M. Cai, O. Painter, and K. J. Vahala, "Observation of critical coupling in a fiber taper to a silica-microsphere whispering-gallery mode system," *Phys. Rev. Lett.*, vol. 85, pp. 74–77, Jul. 2000.

[16] M. Borselli, K. Srinivasan, P. E. Barclay, and O. Painter, "Rayleigh scattering, mode coupling, and optical loss in silicon microdisks," *Appl. Phys. Lett.*, vol. 85, pp. 3693–3695, 2004.

[17] L. Martinez and M. Lipson, "High confinement suspended micro-ring resonators in silicon-on-insulator," *Opt. Express*, vol. 14, no. 13, pp. 6259–6263, Jun. 2006.

[18] S. T. Chu, W. Pan, S. Sato, T. Kaneko, Y. Kokubun, and B. E. Little, "Wavelength trimming of a microring resonator filters by means of a UV sensitive polymer overlay," *IEEE Photon. Technol. Lett.*, vol. 11, no. 6, pp. 688–690, Jun. 1999.

[19] D. K. Sparacin, J. P. Lock, C. Hong, K. K. Gleason, L. C. Kimerling, and J. Michel, "Trimming of microring resonators using photo-oxidation of a plasma-polymerized organosilane cladding material," *Opt. Lett.*, vol. 30, no. 17, pp. 2251–2253, 2005.

[20] W. M. J. Green, R. K. Lee, G. DeRose, A. Scherer, and A. Yariv, "Hybrid InGaAsP-InP Mach-Zehnder racetrack resonator for thermooptic switching and coupling control," *Opt. Exp.*, vol. 13, pp. 1651–1659, Mar. 2005.

[21] M.-C. M. Lee and M. C. Wu, "MEMS-actuated microdisk resonators with variable power coupling ratios," *IEEE Photon. Technol. Lett.*, vol. 17, no. 5, pp. 1034–1036, May 2005.

[22] M.-C. M. Lee and M. C. Wu, "Tunable coupling regimes of silicon microdisk resonators using MEMS actuators," *Opt. Exp.*, vol. 14, no. 11, pp. 4703–4712, May 2006.

[23] U. Levy *et al.*, "On-chip microfluidic tuning of an optical microring resonator," *Appl. Phys. Lett.*, vol. 88, pp. 111107–111109, Mar. 2006.

[24] M.-C. M. Lee and M. C. Wu, "Thermal annealing in hydrogen for 3-D profile transformation on silicon-on-insulator and sidewall roughness reduction," *J. Microelectromech. Syst.*, vol. 15, no. 2, pp. 338–343, Apr. 2006.
[25] J. Yao, M.-C. M. Lee, and M. C. Wu, "Hydrogen annealing and bonding processes for integrated MEMS tunable microtoroidal resonators," to be published.
[26] M.-C. M. Lee, J. Yao, and M. C. Wu, "Silicon profile transformation and sidewall roughness reduction using hydrogen annealing," in *Proc. 18th IEEE Int. Conf. Microelectromech. Syst.*, Miami, FL, Jan. 30–Feb. 3, 2005, pp. 596–599.
[27] J. Yao, M.-C. M. Lee, D. Leuenberger, and M. C. Wu, "Silicon microtoroidal resonators with integrated MEMS tunable optical coupler," in *Proc. IEEE Opt. Microelectromech. Syst.*, Big Sky, MT, 2006, pp. 17–18.
[28] J. Yao, M.-C. M. Lee, D. Leuenberger, and M. C. Wu, "Wavelength- and bandwidth-tunable filters based on MEMS-actuated microdisk resonators," in *Proc. Opt. Fiber Commun. Conf. Nat. Fiber Opt. Eng. Long.*, Anaheim, CA, Mar. 5–10, 2006, p. 3.

Jin Yao received the B.S. and M.S. degrees in electronic engineering from Tsinghua University, China, in 2000 and 2002, respectively. He is currently working toward the Ph.D. degree from the Department of Electrical Engineering and Computer Sciences, University of California, Berkeley.

His current research is focussed on silicon-based integrated microresonators, including design, simulation, fabrication, characterization, and their applications. His research interests include silicon-based photonic integrated circuits and micro-nano scale MEMS.

Mr. Yao won the California NanoSystems Institute (CNSI) Fellowship Award, in 2002–2003.

David Leuenberger received the graduate degree from the Institute of Applied Physics, University of Bern, Switzerland, in 2000. He received the Ph.D. degree from the Swiss Federal Institute of Technology, Lausanne, Switzerland, in 2004.

Currently, he is a Postdoctoral Researcher with the Integrated Photonics Laboratory, University of California, Berkeley. His current research interests include integrated microresonators for optical communication and sensing applications and optical antennas for surface enhanced Raman scattering. He is the author or coauthor of five journal papers and five conference papers.

Dr. Leuenberger is a member of the Optical Society of America (OSA).

Ming-Chang M. Lee (S'04–M'05) was born in Taiwan, R.O.C. He received the B.S. degree in control engineering from the National Chiao Tung University, Hsinchu, Taiwan and the M.S. degree in electrical engineering from the National Taiwan University, Taipei, Taiwan, in 1994 and 1996, respectively. He received the Ph.D. degree in electrical engineering from the University of California, Los Angeles, in 2005.

Currently, he is with the faculty at the Institute of Photonics Technologies and the Department of Electrical Engineering, National Tsing Hua University, Taiwan. His research interests include optical MEMS, studies of nanophotonics, and the development of integrated photonic devices for optical communication and sensing.

Dr. Lee is a member of the Optical Society of America (OSA).

Ming C. Wu (S'82–M'83–SM'00–F'02) received the B.S. degree from National Taiwan University, Taipei, Taiwan, in 1983, and the M.S. and Ph.D. degrees from the University of California, Berkeley, in 1985 and 1988, respectively, all in electrical engineering.

Currently, he is a Professor of electrical engineering and computer sciences at the University of California, Berkeley, and a Co-Director of Berkeley Sensors and Actuators Center (BSAC). From 1988 to 1992, he was a Technical Staff at AT&T Bell Laboratories, Murray Hill, NJ. From 1993 to 2004, he was a Professor of electrical engineering at the University of California, Los Angeles (UCLA). He was also the Director of Nanoelectronics Research Facility and Vice Chair for Industrial Relations during his tenure at UCLA. In 1997, he cofounded OMM in San Diego, CA, to commercialize MEMS optical switches. He has published more than 400 papers, contributed five book chapters, and holds 11 U.S. patents. His research interests include optical MEMS, optoelectronics, and biophotonics. He has also participated in many technical conferences. He was the Guest Editor of two IEEE/OSA JOURNAL OF LIGHTWAVE TECHNOLOGY Special Issues on Optical MEMS.

Dr. Wu was a Fellow of David and Lucile Packard Foundation, from 1992 to 1997. He was the founding Co-Chair of the IEEE/LEOS Summer Topical Meeting on Optical MEMS in 1996.